Unitarity bounds and elastic hadron-hadron scattering in the energy region of the Superconducting Super Collider and beyond

M. Kawasaki
Physics Department, Gifu University, Yanagido, Gifu 501-11, Japan

T. Maehara
Faculty of School Education, Hiroshima University, Hiroshima 734, Japan

M. Yonezawa
Department of Physics, Hiroshima University, Higashi-Hiroshima 724, Japan

(Received 8 June 1993)

The possibility of saturation of unitarity bounds for elastic hadron-hadron scattering at very high energies is discussed with respect to two limits: the MacDowell-Martin and the uniform-disk bounds. The unitarity properties of these two bounds are shown. The analysis by the generalized geometrical scaling model suggests that $\bar{p}p$ elastic scattering first tends to the MacDowell-Martin bound and then turns to the uniform-disk bound as the elasticity becomes larger than ~ 0.4.

PACS number(s): 13.85.Dz, 12.40.Pp

The rising total cross sections of hadron-hadron collisions at high energies [1] showing Froissart-bound-like behavior $\sim(\ln s)^2$ [2] suggest a unitarity-saturating feature of the strong interaction. It is, therefore, interesting to study the unitarity-bound structure of the scattering amplitude in its geometrical aspect. In particular we ask whether or not elastic hadron-hadron scattering will asymptotically approach the MacDowell-Martin bound [3] or the uniform-disk bound [4], which gives the differential cross section

$$\frac{d\sigma}{dt}=(1+\rho^2)\frac{\sigma_t^2}{16\pi}\left[\frac{2^n n!J_n(z)}{z^n}\right]^2,\quad z=R_0\sqrt{-t}\ , \tag{1}$$

where J_n is the Bessel function of the order n, t the squared momentum transfer, R_0 the interaction radius, σ_t the total cross section, and ρ the ratio of the real to the imaginary part of the forward scattering amplitude. The MacDowell-Martin case corresponds to $n=2$ with $R_0=R_{\rm MM}\equiv\sqrt{(1+\rho^2)\sigma_t/3\pi x}$, and the uniform disk $n=1$ with $R_0=R_{\rm UD}=\sqrt{\frac{3}{4}}R_{\rm MM}$, x being the elasticity. The forward logarithmic slope b is given by $b_{\rm MM}\equiv(1+\rho^2)\sigma_t/18\pi x$ for the MacDowell-Martin bound, which is the unitarity lower bound for the slope, and $(\frac{9}{8})b_{\rm MM}$ for the uniform disk.

In this work we show the unitarity properties of these two bounds and give a speculation on whether or not hadron-hadron scattering approaches either of these two limits asymptotically.

The unitarity properties of the bounds can be seen by using the variational solution for the elastic differential cross section under the fixed σ_t, x, and b as well as ρ, with the assumption that the partial-wave amplitude with angular momentum l vanishes for $l>L$ with L being the cutoff angular momentum [5]. The variation gives the extrema of the differential cross section of which asymptotic forms at small momentum transfers are given by [Eq. (20) of Ref. [5]]

$$\frac{d\sigma^{\pm}}{dt}=(1+\rho^2)\frac{\sigma_t^2}{16\pi}\{A(t)\pm\alpha B(t)\}^2\ , \tag{2}$$

with

$$A(t)\equiv(4-12y)A_1-(12-48y)A_3\ , \tag{3}$$

$$B(t)\equiv(A_2-4A_1+24A_1A_3-48A_3^2)^{1/2}\ , \tag{4}$$

$$\alpha\equiv\left[\frac{2}{9}\frac{1}{y_{\rm MM}}-48y^2+24y-4\right]^{1/2}\ , \tag{5}$$

where we have used the notation

$$y=\frac{b}{R_0^2},\quad y_{\rm MM}=\frac{b_{\rm MM}}{R_0^2}\ , \tag{6}$$

$$A_1=\frac{2}{z}J_1(z),\quad A_2=\{J_0(z)\}^2+\{J_1(z)\}^2\ ,$$
$$A_3=\frac{1}{2}\left[\frac{2}{z}J_1(z)-\frac{4}{z^2}J_2(z)\right]\ . \tag{7}$$

Here it is to be noted that $B(t)$ and $dB(t)/dt$ vanish at $t=0$ as expected, but $d^2B(t)/dt^2$ does not. At small momentum transfers $d\sigma^{(+)}/dt$ gives the upper bound, while $d\sigma^{(-)}/dt$ the lower bound.

Now we examine the properties of the partial-wave amplitudes giving these cross sections in order to see the bound structures imposed by unitarity. In the limit of $t\to 0$ the partial-wave amplitude of the solution is given by [6]

$$\mathrm{Im}f_l=\frac{k\sigma_t}{4\pi a_0}\left\{\pm\sqrt{5}\alpha\left[\frac{6}{a_0^2}(l-1)l(l+1)(l+2)-\frac{6}{a_0}l(l+1)+1\right]-\left[(12-48y)\frac{l(l+1)}{2a_0}+12y-4\right]\right\}, \tag{8}$$

and

$$\mathrm{Re}f_l=\rho\,\mathrm{Im}f_l\ , \tag{9}$$

where k is the c.m. system (c.m.s.) momentum and

$$a_0=(L+1)^2,\quad R_0=\frac{L+1}{k}\ . \tag{10}$$

The unitarity condition imposed in the derivation of Eq. (8) is the optical theorem, and the consistency of the solution (8) with the partial-wave unitarity constraint, $0\le k(1+\rho^2)\mathrm{Im}f_l\le 1$, has to be checked for a given set of σ_t, x, b, ρ, and R_0.

Here we ask a question: What restriction is imposed on the interaction radius R_0 from the solution (8)? In the present analysis the only rigorous restriction is obtained from the reality of α. The lowest allowed value of α is zero and in this case the upper and lower bounds coincide and the variation leads to a unique solution, which is quadratic in l and gives the MacDowell-Martin bound solution for $R_0=R_{\mathrm{MM}}$. The condition $\alpha=0$ sets the lower limit for the interaction radius R_0 for given σ_t, σ_{el}, b, and ρ. This is shown in Fig. 1 by a solid curve. As for the upper limit we get no restriction from (8). Some approximate limits may be introduced only with additional assumptions [5]. In Fig. 1 the hatched area is forbidden either by the reality of α or by the well-known MacDowell-Martin bound $b/b_{\mathrm{MM}}\ge 1$.

MacDowell-Martin case. In the limit $b\to b_{\mathrm{MM}}$ the MacDowell-Martin amplitude is the unique solution satisfying the partial-wave unitarity requirement $\mathrm{Im}f_l\ge 0$. This can be shown for the general restriction $x\le\frac{2}{3}$, which is imposed by the unitarity condition for $l=0$. The MacDowell-Martin solution appears at the point $(b/b_{\mathrm{MM}},\ R_0/\sqrt{b_{\mathrm{MM}}})=(1,\sqrt{6})$ and is denoted by MM in Fig. 1. Its partial-wave amplitudes are given by

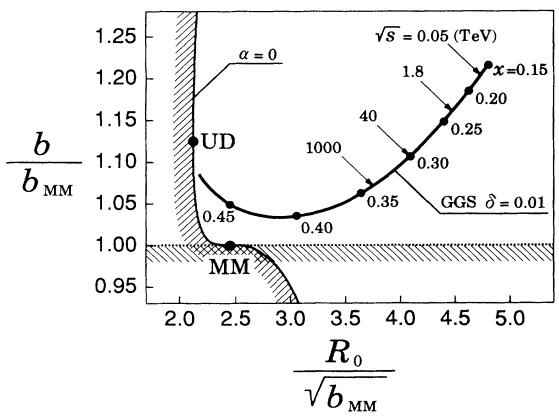

FIG. 1. The hatched area is the forbidden region for b and R_0, of which boundary is given by the conditions $\alpha=0$ and $b/b_{\mathrm{MM}}=1$. The points denoted by MM and UD are the MacDowell-Martin bound and the uniform-disk bound, respectively. The trajectory of GGS is given with the interaction radius defined by the condition $\Delta b/b=\delta=0.01$. Here we have taken the "dipole" eikonal [8] with $\rho=0$.

$$\mathrm{Im}f_l=\frac{k\sigma_t}{2\pi a_0}\left[1-\frac{l(l+1)}{a_0}\right]\quad(0\le l\le L)\ , \tag{11}$$

which provide the differential cross section (1) with $n=2$. This is easily seen, if we take $R_0=R_{\mathrm{MM}}$ and $b=b_{\mathrm{MM}}$ in (2). The solution is characterized by the *minimum* slope $b=b_{\mathrm{MM}}$ as is seen in Fig. 1.

Uniform-disk case. The uniform-disk solution appears at the point $(\frac{9}{8},\sqrt{\frac{9}{2}})$. We have

$$\mathrm{Im}f_l=\frac{k\sigma_t}{4\pi a_0}\quad(0\le l\le L)\ . \tag{12}$$

As is clearly seen in Fig. 1, this solution denoted by UD is the *minimum*-radius bound allowed by the unitarity, and in this sense the uniform disk is the most densely packed solution. The uniform disk is of special interest as a possible asymptotic limit of some high-energy models [4] including the Chou-Yang model [7].

Now we discuss where hadron-hadron scattering is approaching, to either the MacDowell-Martin bound or the uniform-disk bound or elsewhere, as the energy increases over the range reached at the Fermilab Tevatron Collider ($\sqrt{s}=1.8$ TeV) to the CERN Large Hadron Collider (LHC) (15.4 TeV) and the Superconducting Super Collider (SSC) (40 TeV), and further beyond.

As the representative of hadron-hadron scattering, we take $\bar{p}p$ scattering for which the experiments have been performed at the highest energy by the accelerators available so far. In the absence of the experimental data at very high energies, we use the predictions of the generalized geometrical scaling (GGS) model [8,9], which gives a reasonable explanation of the features of the existing experimental data of hadron-hadron scattering in the energy range $\sqrt{s}=10$–1800 GeV [10].

We use the values of the total and elastic cross sections given by the empirical-fit formula

$$\sigma(p)=A+Bp^n+C\ln^2(p)+D\ln(p)$$

(p is the incident laboratory momentum), whose parameters were determined by the data up to 1.8 TeV [11], even above the Tevatron collider energy region. This extrapolation is only to get some idea about the correspondence between the energy $\sqrt{s}$ and the elasticity x and not essential in the following analysis. The essential parameter in the following analysis is the elasticity and we have $x=0.30$ at 40 TeV and 0.34 at 1000 TeV by the extrapolation. Once the elasticity becomes stationary, the only change is geometrical scaling [12,13] under the GGS hypothesis. Further the results obtained for $\bar{p}p$ scattering hold *qualitatively* for all elastic hadron-hadron processes, if the results are interpreted in terms of the elasticity [14].

First we want to draw the trajectory of the GGS prediction on $(b/b_{\mathrm{MM}},R_0/\sqrt{b_{\mathrm{MM}}})$ plane. Realistic models of high-energy hadron-hadron scattering have, however, generally no clear cutoff interaction radii. Here we define an effective radius by requiring that $\Delta Q/Q$ takes some fixed value, where Q is the physical quantity most affected by the cutoff of the interaction at this radius

among those concerned with the present analysis and ΔQ is the change induced by the cutoff. Let $t_{\rm dip}$ be the squared momentum transfers at the first dip of the differential cross section. Of σ_t, $\sigma_{\rm el}$, b, and $t_{\rm dip}$, the forward slope b is most affected by the cutoff and we determine the interaction radius by the condition $|\Delta b/b|=\delta$ for a given value of δ. Naturally this radius increases as δ decreases. We discuss the energy and elasticity variation of this radius.

In Fig. 1 we show the trajectory for $\delta=0.01$. It is to be noted that, if we change the value of δ, any point on the trajectory moves only horizontally; the corresponding value of R_0 changes, while the value of $b/b_{\rm MM}$ remains the same. Here and in the following calculation we neglect the contribution from the real part of the scattering amplitude. The numerical figures attached to the trajectory curve in Fig. 1 are the values of the energy $\sqrt{s}$ and the elasticity x. The obtained curve shows that $\bar{p}p$ scattering is approaching first the MacDowell-Martin bound, then turning to the uniform-disk bound, rather than pointing directly to the uniform-disk point. If the experiments were performed only up to 1000 TeV region, one might conclude that the MM bound would be the asymptotic limit. The radius measured in units of $\sqrt{b_{\rm MM}}$ [15] is rapidly decreasing as x increases. In this sense the interaction is being condensed as the energy increases. Such compactification of the interaction continues as far as x increases to the unitarity limit of the black uniform disk, 0.5.

The preceding arguments rely on a somewhat ambiguous cutoff radius introduced for the GGS amplitude. In the following we make a more direct comparison of the GGS predictions with the MM and UD bounds. In addition to the forward slope, we examine the position of the first dip $t_{\rm dip}$, which also characterizes the cross sections at small momentum transfers. The dip position of the GGS prediction as well as those of MM and UD bounds are shown in Fig. 2.

The ratio $b/b_{\rm MM}$ is steadily decreasing as the energy goes higher from the energy range of the CERN Intersecting Storage Rings (ISR) ($\sim$0.05 TeV). At 1.8 TeV,

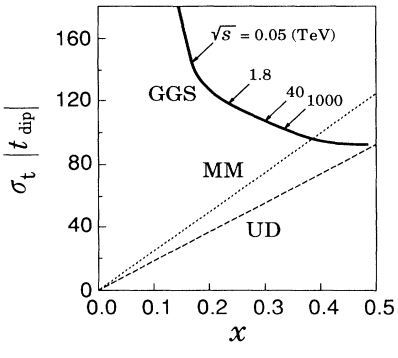

FIG. 2. The dip position $|t_{\rm dip}|$ of the GGS prediction for the "dipole" eikonal [8]. The quantity $\sigma_t|t_{\rm dip}|$ is plotted vs the elasticity x. Here ρ is taken to be zero. The MM and UD lines correspond to the MacDowell-Martin and the uniform disk bound, respectively.

we have $b/b_{\rm MM}=1.160$ by the GGS calculation, which is consistent with the measurements of the slope [16]. This comes near the value of the uniform disk, $9/8=1.125$. The experimental differential cross sections at this energy [17], however, do not show apparent change of the slope in the region $|t|=0$–0.5 (GeV/c)^2, where we expect for the uniform disk the downward curvature of the forward peak and a dip structure. The location of the first dip of the uniform disk is determined by the first zero of $J_1(z)$, $j_{1,1}\approx 3.83$. This gives the position of the dip $t_{\rm dip}$ as

$$\sigma_t|t_{\rm dip}|=\frac{4\pi x}{(1+\rho^2)}(j_{1,1})^2\ , \tag{13}$$

which would imply $|t_{\rm dip}|=0.23$ (GeV/c)^2 for $\sigma_t=74.8$ mb and $\sigma_{\rm el}=17.6$ mb of the empirical fit at 1.8 TeV, while the GGS prediction is 0.62 (GeV/c)^2 and is consistent with the experimental data if the contribution from the real part is taken into account [8,9]. This indicates that the situation is far from the uniform disk as seen in Fig. 1.

As the energy goes higher we pass the point $b/b_{\rm MM}=1.125$ of the uniform-disk value around 14 TeV in the LHC energy range, but the position of the dip of the GGS calculation is far from that of the uniform disk. At 40 TeV of the SSC energy, $b/b_{\rm MM}$ is 1.108, and at 1000 TeV 1.069; therefore, this ratio seems to be approaching the MacDowell-Martin unitarity lower bound monotonically. The first dip of the MacDowell-Martin solution is specified by the first zero of $J_2(z)$, $j_{1,2}\approx 5.14$ as

$$\sigma_t|t_{\rm dip}|=\frac{3\pi x}{(1+\rho^2)}(j_{2,1})^2\ . \tag{14}$$

The GGS prediction at 1000 TeV is $|t_{\rm dip}|=0.20$ (GeV/c)^2 which is compared with 0.17 (GeV/c)^2 of Eq. (14) and 0.13 (GeV/c)^2 of Eq. (13) for the uniform disk. Here we have assumed $\sigma_t=196$ mb and $\sigma_{\rm el}=67$ mb of the empirical formula. The prediction by GGS at this energy is near that of the MacDowell-Martin, but there is some distance to it.

What will happen if the elasticity continues to increase? The ratio $b/b_{\rm MM}$ first decreases to the minimum value ~ 1.03 at around $x=0.4$ and then turns to increase, towards the uniform disk limit. The dip crosses over the MacDowell-Martin value of Eq. (14) near the minimum of $b/b_{\rm MM}$ and approaches the uniform-disk point, as seen in Fig. 2. This movement of the dip position is consistent with the trajectory shown in Fig. 1.

We have shown how elastic hadron-hadron scattering approaches the black uniform disk, if it ever reaches this bound asymptotically. At 40 TeV of the SSC energy region, $\bar{p}p$ scattering ($x=0.3$) will be still far from the asymptotic limit and rather look like pointing to the MacDowell-Martin bound. This is different from the view that the $\bar{p}p$ experimental data at 1.8 TeV indicate the onset of asymptopia [18]. In the sense that each of hadron-hadron scattering processes loses its own identity, the energy where the elasticity reaches ~ 0.35 will be a gate to asymptopia, though the sharp-edge structure of

hadron interaction as in the UD and MM solutions may be discernible at lower elasticity. The interaction radius in units of $\sqrt{b_{\mathrm{MM}}}$ behaves as if becoming *minimally compacted* to the uniform disk at high-energy limit from very expanded states at low energies, though it is ever increasing with the total cross section in the absolute scale. Such a feature is the result of the GGS hypothesis, but qualitatively this feature will be realized more broadly as far as the elasticity increases with the energy [19] and also for all hadron-hadron scattering.

[1] For the experimental behaviors of total and elastic cross sections of hadron-hadron scattering, see Particle Data Group, K. Hikasa *et al.*, Phys. Rev. D **45**, S1 (1992).

[2] M. Froissart, Phys. Rev. **123**, 1053 (1961).

[3] S. W. MacDowell and A. Martin, Phys. Rev. **135**, B960 (1964). The original derivation was carried out for the imaginary part of the scattering amplitude. Here we include also the real part.

[4] See M. M. Block and R. N. Cahn, Rev. Mod. Phys. **57**, 563 (1985).

[5] M. Kawasaki, T. Maehara, and M. Yonezawa, Mod. Phys. Lett. A **7**, 1905 (1992).

[6] In general, the variational solution depends on the scattering angle, but for the purpose of clarifying the unitarity properties of these bounds, the analysis of the forward scattering is sufficient.

[7] T. T. Chou and C. N. Yang, Phys. Rev. **170**, 1591 (1968); L. Durand III and R. Lipes, Phys. Rev. Lett. **20**, 637 (1968).

[8] M. Kawasaki, T. Maehara, and M. Yonezawa, Phys. Rev. D **47**, R3 (1993). See also V. Barger, J. Luthe, and R. J. N. Phillips, Nucl. Phys. **B88**, 237 (1975); T. T. Chou and C. N. Yang, Phys. Lett. B **244**, 113 (1990).

[9] M. Kawasaki, T. Maehara, and M. Yonezawa, Phys. Rev. **D 48**, 3098 (1993).

[10] Previously [8] we used the eikonal obtained by the convolution of two dipole form factors as in the case of the Chou-Yang model [7]. This "dipole" eikonal only explains the experimental data of the differential cross section up to near the first dip, however. The analysis by an eikonal capable of covering the large momentum transfer region has been done in Ref. [9], which shows the previous results are essentially unaltered in the forward peak region. For simplicity we use here also the "dipole" eikonal as in Ref. [8].

[11] See Ref. [1], p. III.83.

[12] J. Dias de Deus, Nucl. Phys. **B59**, 231 (1973); A. J. Buras and J. Dias de Deus *ibid.* **B71**, 481 (1974).

[13] G. Auberson, T. Kinoshita, and A. Martin, Phys. Rev. D **3**, 3185 (1971).

[14] Although there are some definite differences between the form of the eikonal of $\bar{p}p(pp)$ and those of π-p and K-p scattering, they are not to change the results of $\bar{p}p$ qualitatively [9].

[15] The quantity $\sqrt{b_{\mathrm{MM}}}$ or $\sqrt{\sigma_t/x}$ may provide the length scale parameter for the diffractive interaction, M. Kawasaki, T. Takaishi, and M. Yonezawa, Phys. Rev. Lett. **67**, 1197 (1991).

[16] E710 Collaboration, N. A. Amos *et al.*, Phys. Rev. Lett. **68**, 2433 (1992).

[17] E710 Collaboration, N. A. Amos *et al.*, Phys. Lett. B **247**, 127 (1990).

[18] M. M. Block, F. Halzen, and B. Margolis, Phys. Lett. B **252**, 481 (1990).

[19] The rising total cross section implies, in the context of the geometrical picture, the increase of the strength of the eikonal (as in the factorized eikonal model [20]) and/or the expansion of the interaction range of the eikonal (as in the geometrical scaling model [12]). In the former case the elasticity also increases with the total cross section, while it is stationary in the latter case. This basic feature, which is essential in the present analysis, will be qualitatively unchanged, even if the form of the eikonal may change with energy and the generalized geometrical scaling hypothesis may not hold exactly.

[20] H. Cheng, J. K. Walker, and T. T. Wu, Phys. Lett. **44B**, 97 (1973); F. Hayot and U. P. Sukhatme, Phys. Rev. D **10**, 2183 (1974).